Aerosol Science and Technology

ISSN: 0278-6826 (Print) 1521-7388 (Online) Journal homepage: http://www.tandfonline.com/loi/uast20

Factor Analysis of Seattle Fine Particles

Eugene Kim , Philip K. Hopke , Timothy V. Larson , Naydene N. Maykut & Joellen Lewtas

To cite this article: Eugene Kim , Philip K. Hopke , Timothy V. Larson , Naydene N. Maykut & Joellen Lewtas (2004) Factor Analysis of Seattle Fine Particles, Aerosol Science and Technology, 38:7, 724-738, DOI: 10.1080/02786820490490119

To link to this article: http://dx.doi.org/10.1080/02786820490490119

Published online: 17 Aug 2010.

Submit your article to this journal

Article views: 323

View related articles

Citing articles: 36 View citing articles

Full Terms & Conditions of access and use can be found at
http://www.tandfonline.com/action/journalInformation?journalCode=uast20

Download by: [University of North Texas] **Date:** 06 January 2017, At: 01:06

Aerosol Science and Technology, 38:724–738, 2004
Copyright © American Association for Aerosol Research
ISSN: 0278-6826 print / 1521-7388 online
DOI: 10.1080/02786820490490119

Factor Analysis of Seattle Fine Particles

Eugene Kim,[1] Philip K. Hopke,[2] Timothy V. Larson,[3] Naydene N. Maykut,[4] and Joellen Lewtas[5]

[1]*Department of Civil and Environmental Engineering, Clarkson University, Potsdam, NY, USA*
[2]*Department of Chemical Engineering, Clarkson University, Potsdam, NY, USA*
[3]*Department of Civil and Environmental Engineering, University of Washington, Seattle, WA, USA*
[4]*Puget Sound Clean Air Agency, Seattle, WA, USA*
[5]*Human Exposure and Atmospheric Sciences Division, National Exposure Research Laboratory, US EPA, Port Orchard, WA, USA*

Ambient particulate matter $\leq$2.5 μm in aerodynamic diameter ($PM_{2.5}$) samples were collected at a centrally located urban monitoring site in Seattle, WA on Wednesdays and Saturdays using Interagency Monitoring of Protected Visual Environments (IMPROVE) samplers. Particulate carbon was analyzed using the thermal optical reflectance method that divides carbon into four organic carbon (OC), pyrolyzed organic carbon (OP), and three elemental carbon (EC) fractions. A total of 384 samples that were analyzed for 36 species were collected between March 1996 and February 2000. These data were analyzed with the standard factor analysis model using the Multilinear Engine (ME). Eleven sources were identified: sulfate-rich secondary aerosol (26%), diesel emissions (22%), wood smoke (16%), gasoline vehicle (10%), aged sea salt (8%), airborne soil (7%), nitrate-rich secondary aerosol (5%), sea salt (4%), oil combustion (3%), paper mill (2%), and ferrous metal processing (1%). The use of ME provided enhanced source separations, including the nitrate-rich aerosol source and two industrial sources that were not deduced in a previous PMF2 solution. Conditional probability functions using surface wind data and resolved source contributions aid in the identifications of local sources. Potential source contribution function analysis tentatively shows southern Washington State, along the Canadian border, and southwestern British Colombia, Canada as the possible source areas and pathways that give rise to the high contribution of the sulfate-rich secondary aerosol.

Received 23 October 2003; accepted 26 May 2004.

Present address of Joellen Lewtas: Department of Environmental and Occupational Health Sciences, University of Washington, Box 354803, Seattle, WA 98195.

This study was funded by University of Washington/EPA Northwest Research Center for Particulate Air Pollution and Health (R827355) and by University of Rochester/EPA Particulate Matter and Health Center (R827354). This support does not constitute an endorsement by U.S. EPA of the views expressed. The authors acknowledge the NOAA Air Resources Laboratory (ARL) for the provision of the HYSPLIT transport and dispersion model and READY website (http://www.arl.noaa.gov/ready.html) used in this publication.

Address correspondence to Philip K. Hopke, Department of Chemical Engineering, Clarkson University, Box 5708, Potsdam, NY 13699, USA. E-mail: hopkepk@clarkson.edu

INTRODUCTION

Source apportionment studies for airborne particulate matter (PM) are needed with an increased focus on the control of the sources of airborne PM, since U.S. Environmental Protection Agency promulgated new national ambient air quality standards for airborne PM. Positive matrix factorization (PMF) (Paatero 1997) and Unmix (Henry and Norris 2002) have been shown to be powerful alternatives to traditional multivariate receptor modeling of airborne PM (Huang et al. 1999; Willis 2000; Qin et al. 2002; Maykut et al. 2003). PMF has been used to assess particle source contributions in Phoenix (Ramadan et al. 2000), in Vermont (Polissar et al. 2001a), in three northeastern U.S. cities (Song et al. 2001), and in Atlanta (Kim et al. 2003a). Unmix has been applied to several aerosol data sets from Los Angeles (Kim and Henry 2000) and Phoenix (Lewis et al. 2003). Also, PMF and Unmix were compared in the northern Vermont aerosol study (Poirot et al. 2001) and in the Seattle aerosol study (Maykut et al. 2003).

A more flexible tool to fit multilinear models, the multilinear engine (ME: Paatero 1999), was developed in order to solve any problem that can be expressed as a sum of product terms (e.g., Equation (1)). It has been used to analyze the standard bilinear factor analysis model (Ramadan et al. 2003) and multiway models (Xie et al. 1999; Yli-Tuomi et al. 2003; Hopke et al. 2003; Kim et al. 2003b).

The objective of this study is to examine the use of ME with the standard bilinear model for identifying particulate matter $\leq$2.5 μm in aerodynamic diameter ($PM_{2.5}$) sources and estimating their contributions to $PM_{2.5}$ mass concentrations. In the present study, ME was applied to an ambient $PM_{2.5}$

compositional data set of 24 h integrated samples, including 8 individual carbon fractions collected during a 3 year period at the Interagency Monitoring of Protected Visual Environments (IMPROVE) (Malm et al. 1994) monitoring site in Seattle, WA. The resolved $PM_{2.5}$ particle sources and their seasonal trends are discussed. The results of this study were compared with the results of a previous chemical mass balance (CMB) study (Chow et al. 1998) and a two-way PMF (PMF2) study (Maykut et al. 2003).

EXPERIMENTAL

Sample Collection and Chemical Analysis

The $PM_{2.5}$ compositional data analyzed in this study consisted of samples taken on Wednesdays and Saturdays at the IMPROVE monitoring site (Beacon Hill) located in Seattle, Washington. As shown in Figure 1, the Beacon Hill monitoring site is centrally located within the Seattle urban area on a hilltop, 99 m above sea level. The monitoring site is located inside a water reservoir impoundment, located 5 km southeast of the downtown business district. The area to the immediate north and east of the reservoir is residential. The hill is part of a larger ridge defining the eastern edge of an industrialized valley. The Port of Seattle, and container shipping and warehousing areas are located northwest and west of the site. Highways having a traffic count of approximately 2×10^5 vehicles per day (Washington State Department of Transportation 2002) are closely situated about 2 km north and 1 km west of the site. The Pacific Ocean is located approximately 150 km west of the site, and Puget sound is located immediately west of the site. Wind data were measured on a 10 m tower located at the site. The prevailing winds at the monitoring site were from the southwest (24%), northwest (13%), and northeast (18%). The highest wind speeds (upper 25%) were from the southwest (56%).

Integrated 24 h $PM_{2.5}$ samples were collected on Teflon, Nylon, and quartz filters. The Teflon filter was used for mass concentrations and analyzed via particle-induced X-ray emission (PIXE) for Na to Mn, X-ray fluorescence (XRF) for Fe

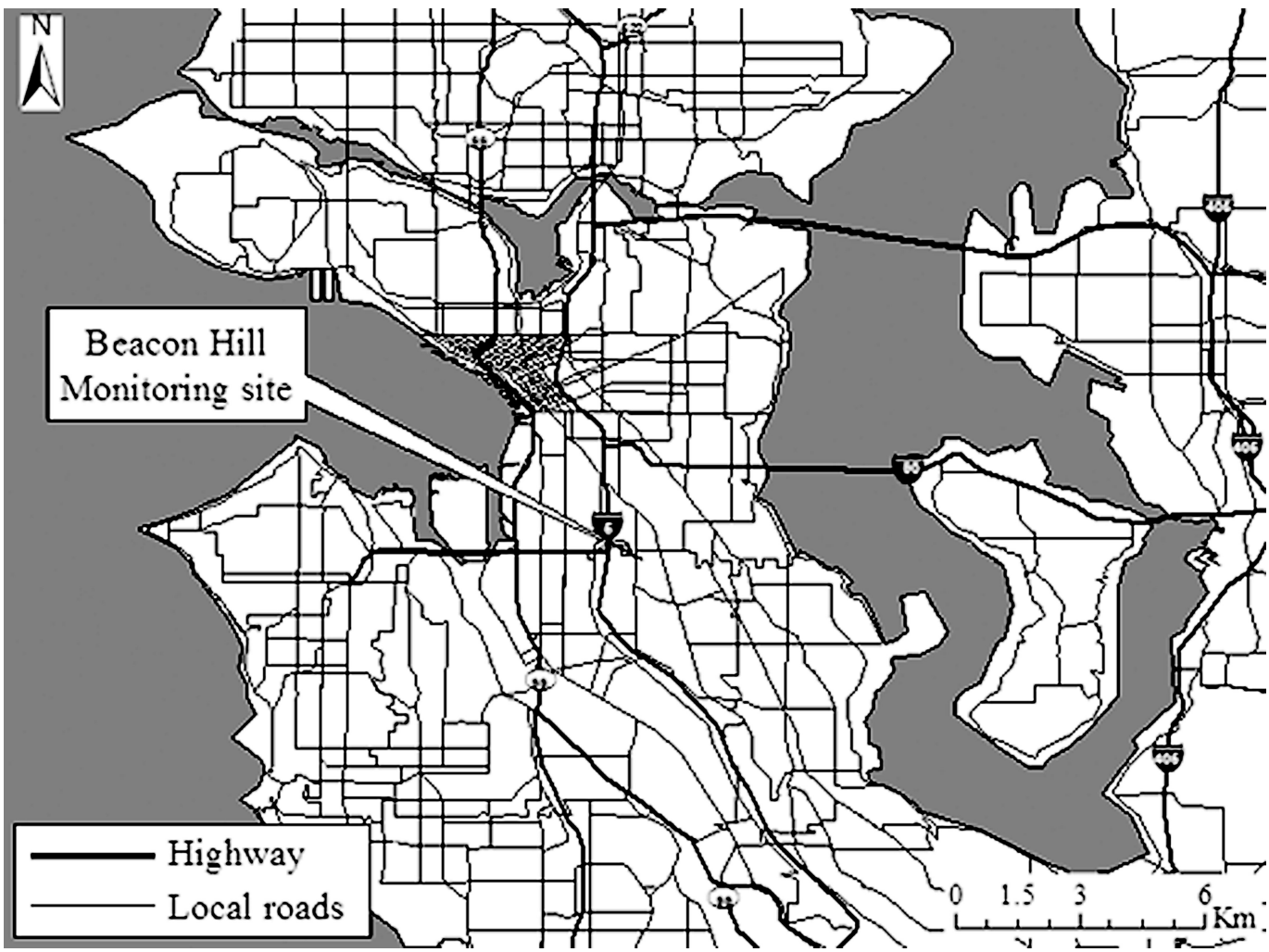

Figure 1. Location of the IMPROVE monitoring site in Seattle, WA.

to Pb, proton elastic scattering analysis (PESA) for elemental hydrogen concentration at University of California at Davis, CA (Cahill et al. 1987). The Nylon filter was analyzed via ion chromatography (IC) for sulfate ($SO_4^=$), nitrate (NO_3^-), nitrite (NO_2^-), and chloride (Cl^-) at Research Triangle Institute, Research Triangle Park, NC. The quartz filter was analyzed via thermal optical reflectance (TOR) protocol (Chow et al. 1993) for 8 temperature-resolved carbon fractions (Desert Research Institute, Reno, NV). This protocol volatilizes organic carbon (OC) by four temperature steps in a helium atmosphere: OC1 at 120°C, OC2 at 250°C, OC3 at 450°C, and OC4 at 550°C. After OC4 response returns to baseline or a constant value, the pyrolyzed organic carbon (OP) is oxidized at 550°C in a mixture of 2% oxygen and 98% helium atmosphere prior to the return of reflectance to its original value. Then three elemental carbon (EC) fractions are measured in oxidizing atmosphere: EC1 at 550°C, EC2 at 700°C, and EC3 at 850°C.

Samples for which $PM_{2.5}$ mass concentrations were not available or all 8 carbon fractions were not available were excluded from this analysis. Samples in which the $PM_{2.5}$ mass concentration error flag was not "NM" (normal) were also not included in this study. XRF sulfur and $SO_4^=$ showed excellent correlations ($slope = 2.7 \pm 0.03$, $r^2 = 0.95$), so $SO_4^=$ was excluded from the analysis. The reported EC1 concentration in IMPROVE/TOR protocol includes the OP concentration. In this study, the OP was subtracted from EC1 and utilized as an independent variable. EC1 in this study did not include OP. Thus, a total of 384 samples collected between March 1996 and February 2000 and 36 species were used in this study. A summary of the $PM_{2.5}$ speciation data used in this study is given in Table 1.

Data Analysis

The general receptor modeling problem can be stated in terms of the contribution from p independent sources to all chemical species in a given sample as follows (Miller et al. 1972; Hopke 1985):

$$x_{ij} = \sum_{k=1}^{p} g_{ik} f_{kj} + e_{ij}, \qquad [1]$$

where x_{ij} is the jth species concentration measured in the ith sample, g_{ik} is the particulate mass concentration from the kth source contributing to the ith sample, f_{kj} is the jth species mass fraction from the kth source, e_{ij} is residual associated with the jth species concentration measured in the ith sample, and p is the total number of independent sources. To solve a variety of receptor modeling problems, ME provides a new approach to the fitting process that is more general and flexible (Paatero 1999). ME uses a structural equation input along with a set of constraints and can solve widely different multilinear and quasi-multilinear problems. In this study, ME solved the standard bilinear model in Equation (1). There are an infinite number of possible solutions to the factor analysis problem due to the free rotation of matrices (Henry 1987). To decrease this rotational freedom, both ME and PMF2 use nonnegativity constraints on the factors (Paatero 1997, 1999). However, they use different algorithms to obtain the least-square solution and the nonnegativity constrains are imposed in different ways. Both ME and PMF2 provide a solution that minimizes an object function, $Q(E)$, based upon uncertainties for each observation (Paatero 1999). This function is defined as

$$Q(E) = \sum_{i=1}^{n} \sum_{j=1}^{m} \left[\frac{x_{ij} - \sum_{k=1}^{p} g_{ik} f_{kj}}{u_{ij}} \right]^2, \qquad [2]$$

where u_{ij} is an uncertainty estimate in the jth constituent measured in the ith sample.

In ME, the factor analysis problem is solved by using a modified form of the preconditioned Conjugate Gradient algorithm instead of Newton-Raphson method that is used in PMF. Also, constraints are imposed in ME as in traditional nonnegative least squares (hard constraints) rather than using the penalty function approach (softer constraint) in PMF. It is also easy to add additional constraints in ME, but this is not possible in PMF.

The application of ME depends on the estimated uncertainties for each of the data values. The uncertainty estimation provides a useful tool to decrease the weight of missing and below-detection-limit data in the solution. The procedure of Polissar et al. (1998) was used to assign measured data and the associated uncertainties as the input data to the ME. The concentration values were used for the measured data, and the sum of the analytical uncertainty and 1/3 of the detection limit value was used as the uncertainty assigned to each measured value. Values below the detection limit were replaced by half of the detection limit values, and their uncertainties were set at 5/6 of the detection limit values. Missing values were replaced by the geometric mean of the measured values, and their accompanying uncertainties were set at four times this geometric mean value.

The uncertainty must take into account both the measurement uncertainty and the temporal variability in the source profiles. In this study, it was found necessary to increase the estimated uncertainties of Al and K by a factor of two and three, respectively, to take the high variability into account so that the larger uncertainties decreased their weight in the model fit (Paatero and Hopke 2003). The estimated uncertainties of OC1 were increased by a factor of two to reduce the influence of the known positive artifact from the adsorption of gaseous OC (Pankow and Mader 2001), and the estimated uncertainties of EC1 were increased by a factor of two to account for the additional uncertainty from the subtraction of OP.

The results of ME were then normalized by a scaling constant, s_k, so that the quantitative source contributions as well as profiles for each source were obtained. Specifically,

$$x_{ij} = \sum_{k=1}^{p} (s_k g_{ik}) \left(\frac{f_{kj}}{s_k} \right), \qquad [3]$$

Table 1
Summary of $PM_{2.5}$ and 36 species mass concentrations used for ME analysis

Species	Concentration (ng/m^3)				Number of BDL values (%)	Number of missing values (%)
	Arithmetic mean	Geometric mean[a]	Minimum	Maximum		
$PM_{2.5}$	8749	7600	1905	33368	0	0
OC1	428	298	6.7	3433	50 (13.0)	0
OC2	625	525	126	2876	0	0
OC3	986	792	149	5597	0	0
OC4	806	637	151	5147	0	0
OP	93	41	2.9	1868	273 (70.7)	0
EC1	1030	821	115	5813	0	0
EC2	65	47	2.9	260	164 (42.5)	0
EC3	18	14	1.5	99	287 (74.4)	0
S	497	402	52	1833	0	0
NO_2^-	12	11	0.20	68	343 (88.9)	26 (6.8)
NO_3^-	551	458	52	2399	0	26 (6.8)
Al	68	49	6.1	695	226 (58.5)	0
As	1.1	0.90	0.20	5.9	157 (40.7)	0
Br	2.9	2.4	0.38	20	1 (0.3)	0
Ca	43	38	11	223	0	0
Cl	341	179	3.2	2564	267 (69.2)	0
Cl^-	216	88	0.30	1619	155 (40.2)	26 (6.8)
Cr	3.3	2.9	0.85	13	155 (40.2)	0
Cu	3.5	2.3	0.52	158	4 (1.0)	0
Fe	78	61	12	459	0	0
H	349	287	88	1717	0	0
K	58	50	13	219	0	0
Mg	65	43	7.6	349	350 (90.7)	0
Mn	8.8	6.0	0.92	91	120 (31.1)	0
Na	313	235	17	2332	13 (3.4)	0
Ni	1.8	1.1	0.12	13	105 (27.2)	0
P	24	19	9.6	38	382 (99.0)	0
Pb	6.7	4.9	0.84	74	0	0
Rb	0.27	0.24	0.09	0.93	264 (68.4)	0
Se	0.61	0.41	0.06	5.6	118 (30.6)	0
Si	83	63	7.3	947	2 (0.5)	0
Sr	0.65	0.53	0.10	5.5	48 (12.4)	0
Ti	7.5	6.3	0.84	27	90 (23.3)	0
V	6.6	5.0	0.69	46	127 (32.9)	0
Zn	12	9.7	1.7	61	0	0
Zr	0.25	0.20	0.07	0.68	345 (89.4)	0

[a]Data below the limit of detection were replaced by half of the reported detection limit values for the geometric mean calculations.
BDL, below detection limit.

where s_k is determined by regressing total $PM_{2.5}$ mass concentrations in the ith sample, m_i, against estimated source contribution values:

$$m_i = \sum_{k=1}^{p} s_k g_{ik}. \quad [4]$$

Conditional Probability Function

The conditional probability function (CPF; Kim et al. 2003a) analyzes point source impacts from varying wind directions using the source contribution estimates from ME coupled with the wind directions measured on site. The CPF estimates the probability that a given source contribution from a given wind direction will exceed a predetermined threshold

criterion. The same daily contribution was assigned to each hour of a given day to match to the hourly wind data. The CPF is defined as

$$\mathrm{CPF} = \frac{m_{\Delta\theta}}{n_{\Delta\theta}}, \quad [5]$$

where $m_{\Delta\theta}$ is the number of occurrence from wind sector $\Delta\theta$ that exceeded the threshold criterion, and $n_{\Delta\theta}$ is the total number of data from the same wind sector. In this study, 32 sectors were used ($\Delta\theta = 11.25$ degrees). Calm winds (<1 m/s) were excluded from this analysis due to the isotropic behavior of wind vane under calm winds. From the tests with several different percentile of the fractional contribution from each source, the threshold criterion of upper 30% was chosen to show the directionality of the sources clearly. The sources that have high conditional probability values are likely to be located to the direction.

Potential Source Contribution Function

To estimate regional source impacts for the sulfate-rich secondary aerosol, the potential source contribution functions (PSCF; Ashbaugh et al. 1985; Hopke et al. 1995) was calculated using source contribution estimated from ME as well as backward trajectories reconstructed by the Hybrid Single Particle Lagrangian Integrated Trajectory (HYSPLIT) model (Draxler and Rolph 2003; Rolph 2003). Three-day backward trajectories starting at height of 500 m above the ground level were computed every day, producing 72 trajectories per sample. The geophysical region covered by the trajectories was divided into 3542 grid cells of $1^\circ \times 1^\circ$ latitude and longitude so that there are an average of 8 trajectory endpoints per cell. If a trajectory endpoint of the air parcel lies in the *ij*th cell, the trajectory is assumed to collect $PM_{2.5}$ emitted in the cell. Once the $PM_{2.5}$ is incorporated into the air parcel, it is assumed to be transported along the trajectory to the monitoring site. PSCF_{ij} is the conditional probability that an air parcel that passed through the *ij*th cell had a high concentration upon arrival at the monitoring site defined as

$$\mathrm{PSCF}_{ij} = \frac{m_{ij}}{n_{ij}}, \quad [6]$$

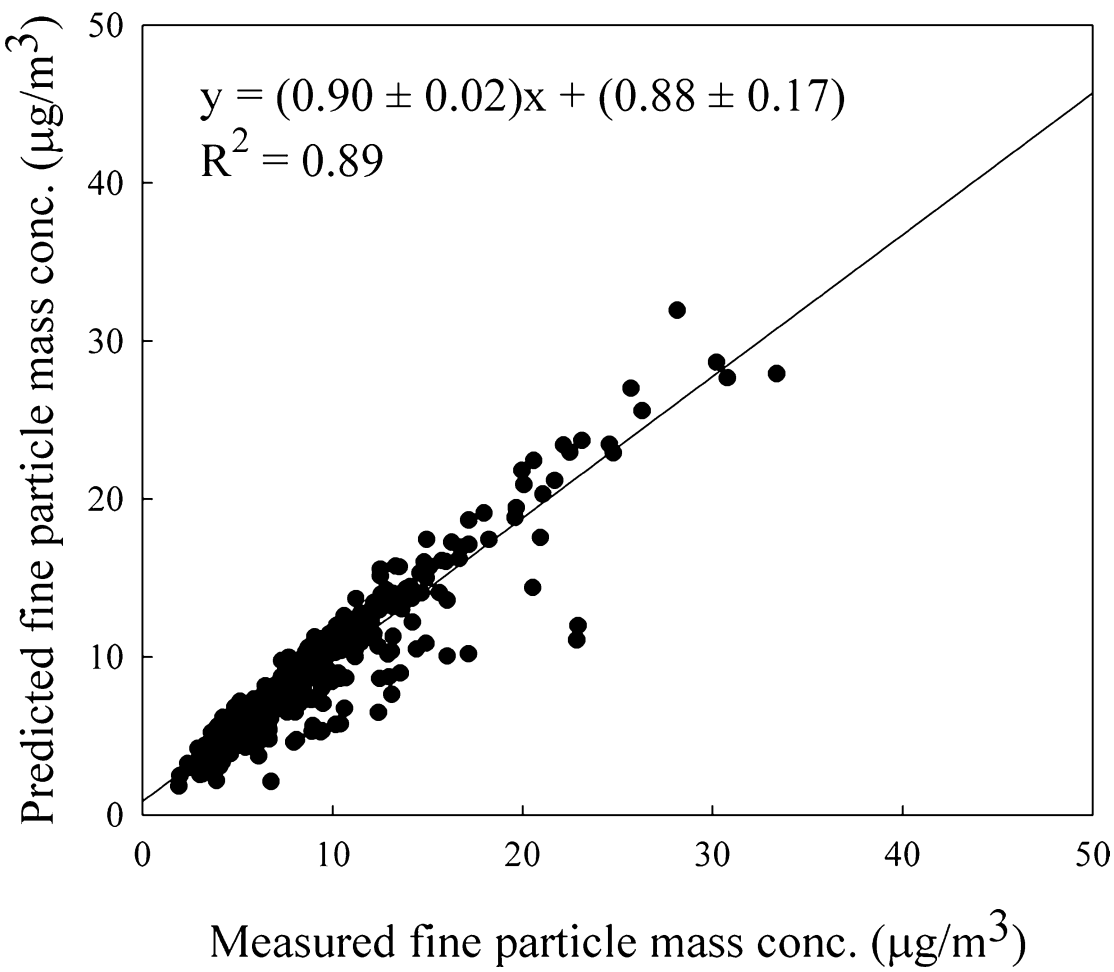

Figure 2. Measured versus predicted $PM_{2.5}$ mass concentration.

where n_{ij} is the total number of endpoints that fall in the ijth cell and m_{ij} is the number of endpoints in the same cell that are associated with samples that exceeded the threshold criterion. In this study, the average contribution of each source was used for the threshold criterion. The sources are likely to be located in the areas that have high PSCF values.

To minimize the effect of small values of n_{ij} that result in high PSCF values with a high uncertainties, an arbitrary weight function $W(n_{ij})$ was applied to downweight the PSCF values for the cell in which the total number of endpoints was less than three times the average number of the endpoints per cell (Hopke et al. 1995; Polissar et al. 2001b):

$$W(n_{ij}) = \begin{cases} 1.0 & 24 < n_{ij} \\ 0.7 & 3 < n_{ij} \leq 24 \\ 0.4 & 2 < n_{ij} \leq 3 \\ 0.2 & 2 \leq n_{ij} \end{cases} . \quad [7]$$

RESULTS AND DISCUSSION

To determine the number of sources, it is necessary to test different numbers of sources and find the optimal fit with the most physically reasonable results. The robust mode was used to reduce the influence of extreme values on the ME solution. A data point was classified as an extreme value if the residual exceeded four times the error estimate in the process of model iterations. The estimated uncertainties of those extreme values were then increased so that the weights of the extreme values in the solution were decreased. The final solutions were determined by experiments with different numbers of sources and different uncertainties for downweighting with the final choice based on the evaluation of the resulting source profiles as well as the quality of the individual species fits. The global optimum of the ME solutions were tested by using multiple random starts for the initial values used in the iterative fitting process (Paatero 2000). In the eleven-source solution, a factor is observed that appears to be a likely source and was not present in the ten-source solution. In twelve-source model, one factor was separated to two factors in a way that was not reasonable, and thus the eleven-solution model was selected.

As shown in Figure 2, a comparison of the daily reconstructed $PM_{2.5}$ mass contributions from all sources with measured $PM_{2.5}$ mass concentrations indicates that the resolved sources effectively reproduce the measured values and account for most of the variation in the $PM_{2.5}$ mass concentrations (*slope* $= 0.90 \pm 0.02$, *intercept* $= 0.88 \pm 0.17$, and $r^2 = 0.89$). This shows improvement in model predictions when the slopes and intercepts are compared with those from previous PMF analysis (*slope* $= 0.87 \pm 0.02$, *intercept* $= 1.20 \pm 0.20$, and $r^2 = 0.88$). The identified source profiles are presented in Figure 3. Figure 4 presents time series plots of estimated daily contributions from each source to $PM_{2.5}$ mass concentrations. In Figure 5, the averaged seasonal contributions from each source are presented (summer, April–September, winter, October–March). The observed seasonal variations may be due to variation in source strength or in transport condition or in both. The average source contributions of each source to the $PM_{2.5}$ mass concentrations are compared in Table 2 to the previous CMB study analyzing measurements from 1996 to 1997 and the PMF2 study analyzing measurements from 1996 to 1999.

Sulfate-rich secondary particles have high concentrations of S and provide the highest contribution to $PM_{2.5}$ mass concentrations (26%). Secondary aerosols typically become associated with carbon and tracer elements (Liu et al. 2003). This association is consistent with previous studies that observed similar profiles in the data from eastern U.S. (Song et al. 2001; Kim et al. 2003a, 2004), although the total contribution in Seattle is about 50% of those observed in the eastern U.S. As shown in Figures 4 and 5, the sulfate-rich secondary aerosol shows strong seasonal variation, with higher concentrations in summer when the photochemical activity is highest (Polissar et al. 2001a; Song et al. 2001). The average source contributions from sources to

Table 2
The comparison of average source contribution ($\mu g/m^3$) to $PM_{2.5}$ mass concentrations among CMB (Chow et al. 1998), PMF2 (Maykut et al. 2003), and this study using ME

	Average source contribution (standard error)		
	CMB[a]	PMF2[b]	ME[c]
Secondary aerosol		1.6 (0.07)	
Sulfate aerosol	1.7		
Sulfate-rich secondary aerosol			2.2 (0.10)
Nitrate-rich secondary aerosol			0.4 (0.02)
Motor vehicle	3.2		
Gasoline vehicle		0.4 (0.03)	0.8 (0.06)
Diesel emissions		1.6 (0.1)	1.9 (0.10)
Sea salt		0.3 (0.04)	0.3 (0.04)
Aged sea salt		0.4 (0.02)	0.7 (0.03)
$NaNO_3$	0.8		
Marine	0.3		
Vegetative burning/cooking	1.8		
Wood smoke		2.5 (0.2)	1.4 (0.09)
Airborne soil	0.3	1.2 (0.08)	0.6 (0.03)
Oil combustion	0.1	0.9 (0.07)	0.2 (0.02)
Paper mill	0.1		0.2 (0.01)
Metal processing	0.2		0.1 (0.005)

[a]Chow et al. (1998).
[b]Maykut et al. (2003).
[c]This study.

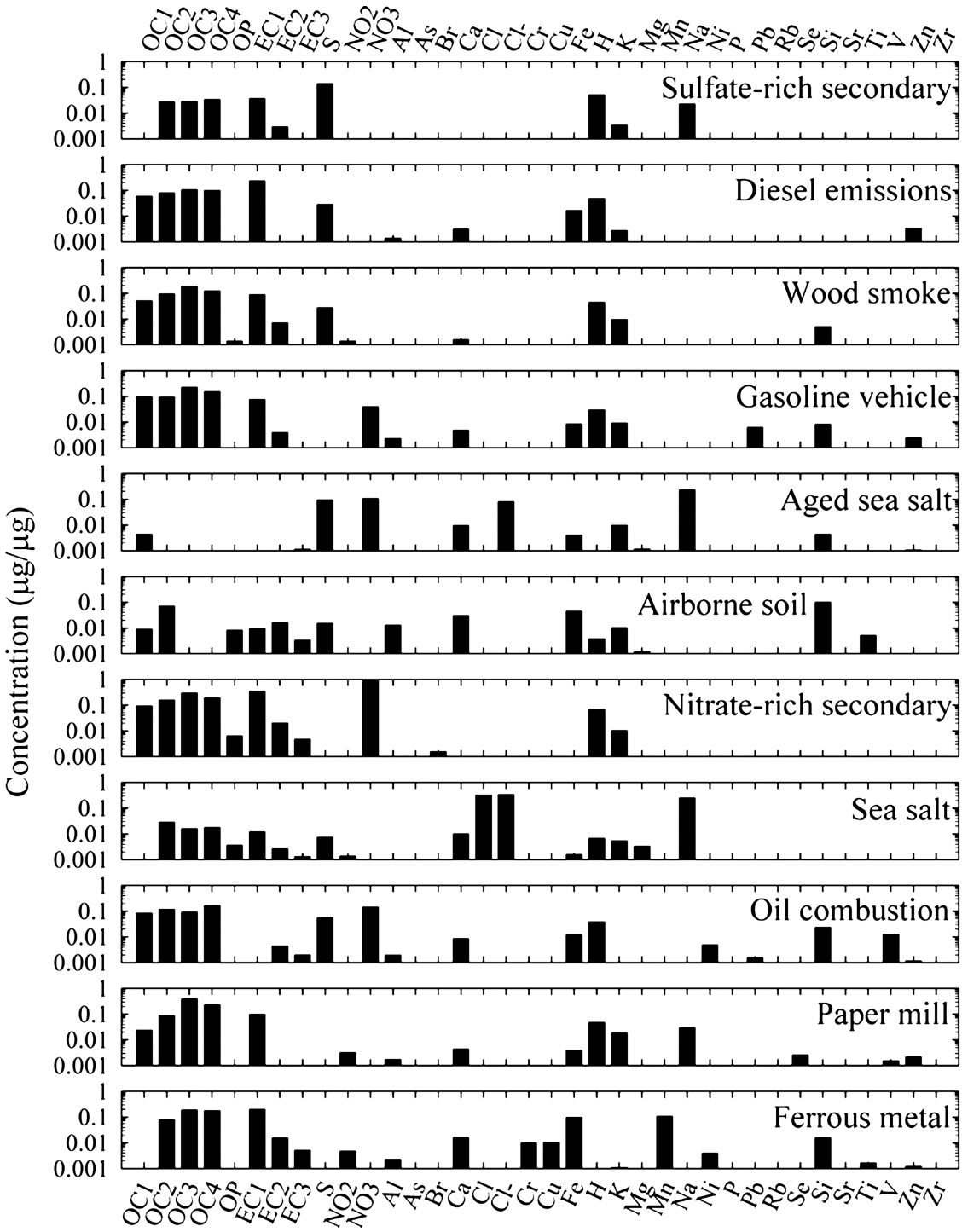

Figure 3. Source profiles deduced from $PM_{2.5}$ samples.

the $PM_{2.5}$ mass contributions are compared between weekday and weekend in Figure 6. The sulfate-rich secondary aerosol does not show weekday/weekend variations, reflecting its nature of regional transport. The averaged contribution of 2.2 $\mu g/m^3$ from the sulfate-rich secondary aerosol to the $PM_{2.5}$ mass concentration is consistent with 2.3 $\mu g/m^3$ of sulfate-rich secondary aerosol identified in Spokane, WA (Kim et al. 2003c). The prior PMF2 study (Maykut et al. 2003) resolved 1.6 $\mu g/m^3$ contribution of secondary aerosol, including sulfate-rich and nitrate-rich aerosols. An earlier CMB study (Chow et al. 1998) resolved 1.7 $\mu g/m^3$ contribution of sulfate aerosol that did not include secondary organics.

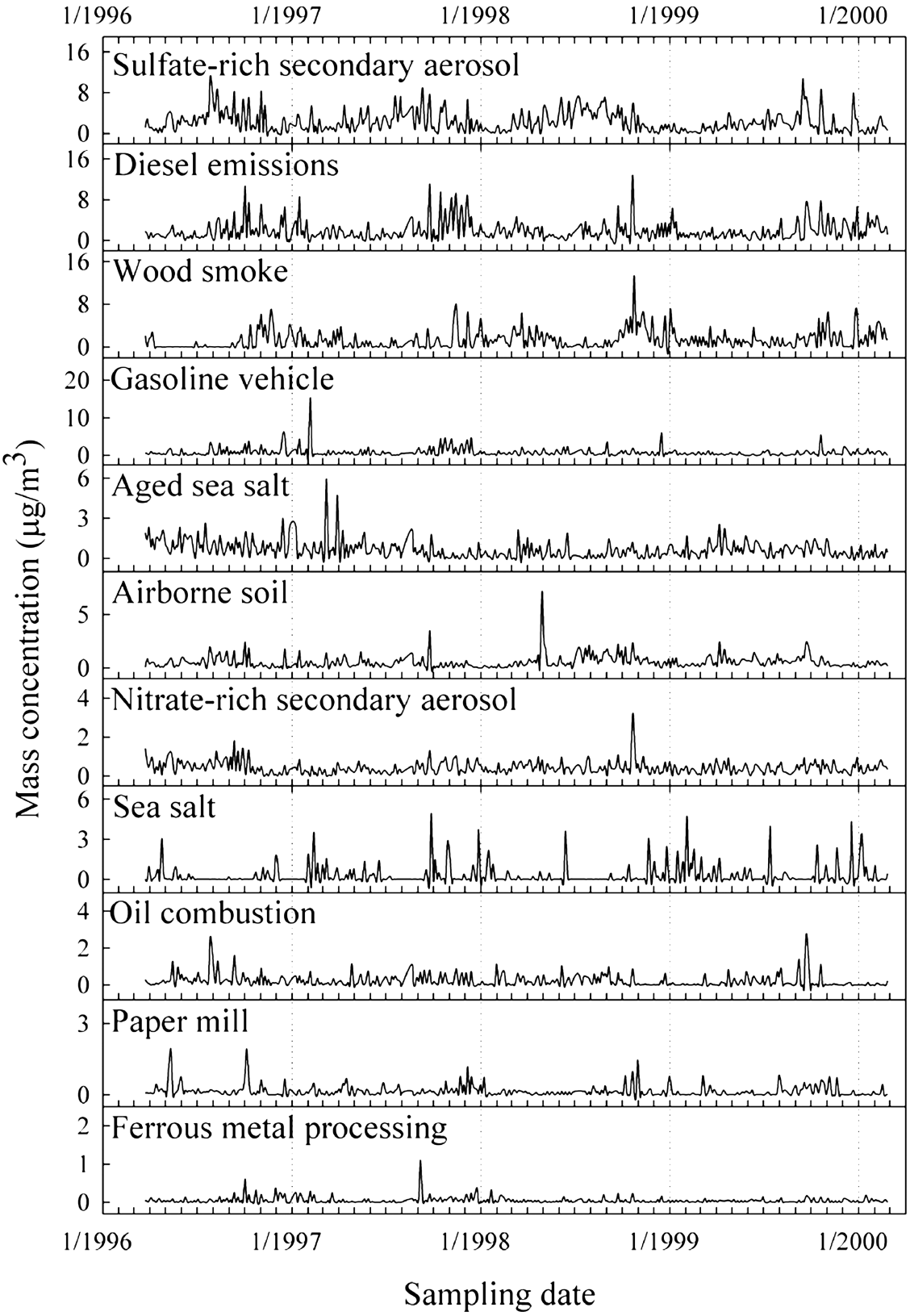

Figure 4. Time series plot of source contributions.

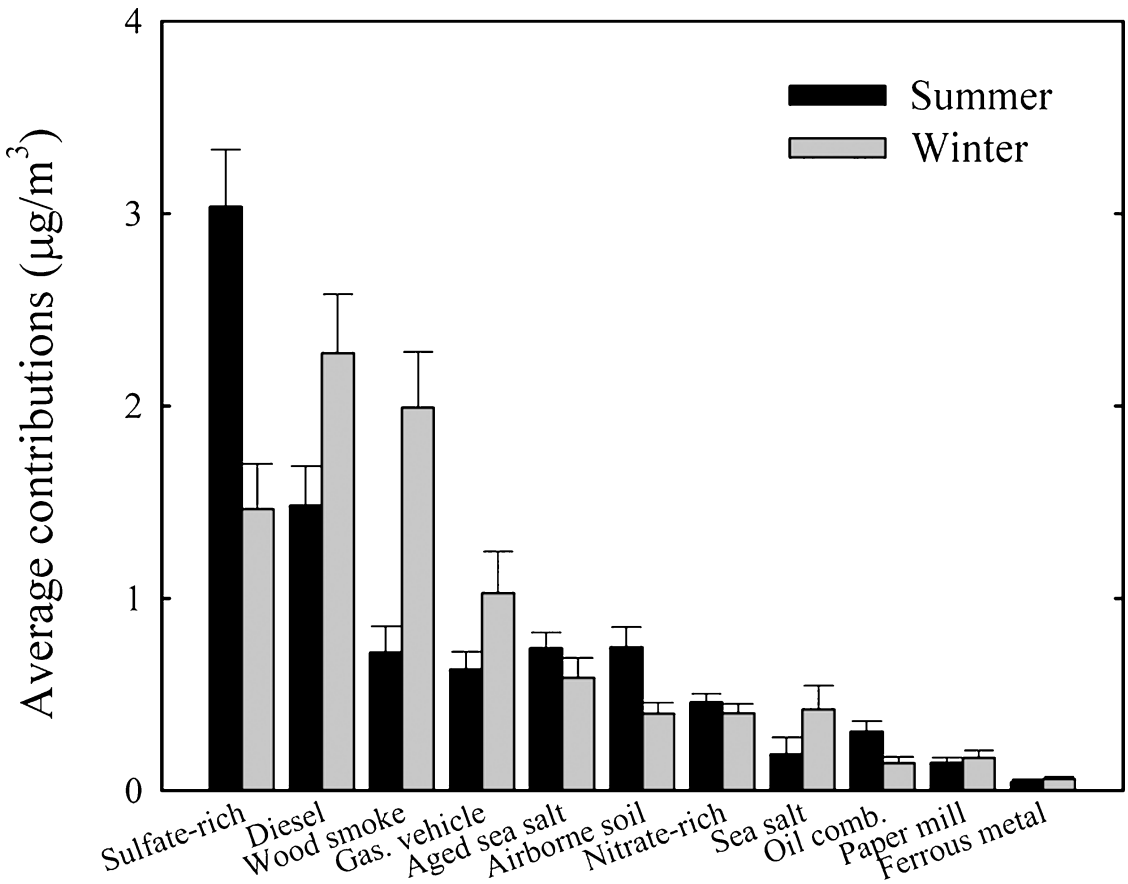

Figure 5. The seasonal comparison of source contributions to $PM_{2.5}$ mass concentration (mean ± 95% confidence interval).

As shown in Figure 7, the PSCF plot of this source shows high values in southern Washington, along the Canadian border, and in southwestern British Colombia, Canada as potential source areas and pathways that give rise to the high contribution to the Beacon Hill monitoring site. These identified areas also include areas where the sulfate-rich secondary aerosol is formed in addition to areas where the sources are located. The high PSCF values that lie in southern Washington State could be related to emissions from coal-fired, electricity-generating plants located between Washington and Oregon. In contrast, the region with a coal-fired, electricity-generating plant located 90 km south of the monitoring site has low PSCF values, indicating the emissions from this source are too close to provide the time required for secondary formation. Also, this region is a favored upwind region in the winter when secondary formation is suppressed. The PSCF plot indicates regional influences from the areas where industries and coal-fired power plants are located. However, the HYSPLIT model (Draxler and Rolph 2003; Rolph 2003) is not accounting for terrain effects that are important in the northwest region, and therefore these results are preliminary and warrant further study with alternative trajectory models.

Gasoline vehicle and diesel emissions have high concentrations of the carbon fractions whose abundances differ between the source types. Gasoline vehicles and diesel emissions account for 10% and 22% of the $PM_{2.5}$ mass concentration, respectively. In the PMF2 analysis (Maykut et al. 2003), gasoline vehicle and diesel emissions account for 4% and 18%, respectively. The ME extracted fractional carbon profiles for the 4 main combustion sources are presented in Figure 8. Gasoline vehicles emissions have high OC fractions concentrations. In contrast, diesel emissions contain high concentrations of EC. These are consistent with previous measurements (Watson and Chow 2001; Watson et al. 1994, 2001; Lowenthal et al. 1994). Specifically, the gasoline vehicle emissions has large amounts of OC3 and OC4. Diesel emissions contain high concentrations of EC1. These results are similar to those estimated in an Atlanta aerosol study including 8 carbon fractions (Kim et al. 2004). However, the contribution from the highly emitting gasoline vehicles, which has high concentration of EC1, can be included in the diesel emissions.

In Figure 9, conditional probabilities of source directions for each source are plotted in polar coordinates. The highest CPF values of gasoline vehicle source points are to the west, which is the direction of closely located highway junction. Diesel emissions appears to have contributions mostly from west and northwest where highway junction and Port of Seattle are

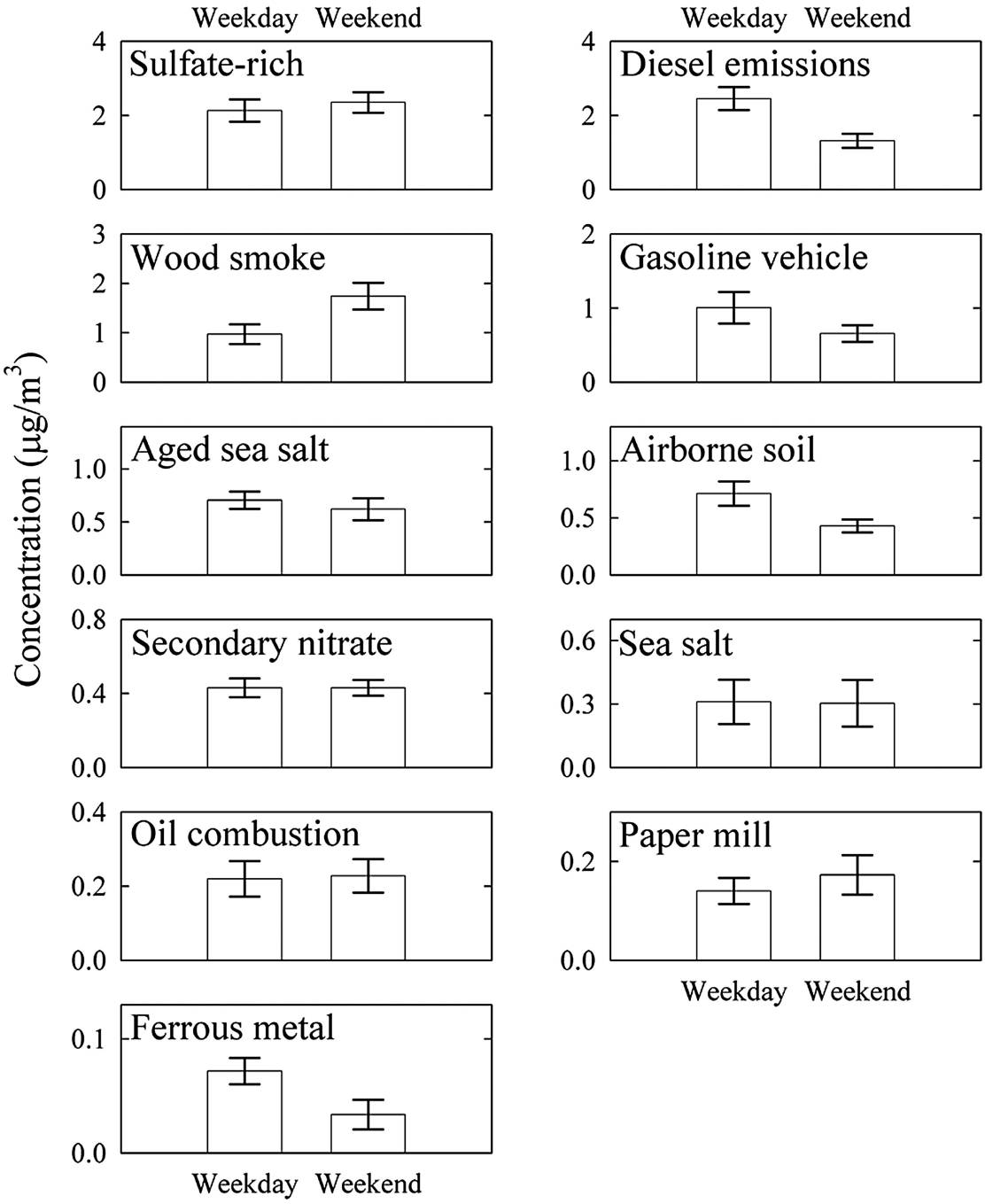

Figure 6. The comparisons of model resolved contributions between weekday and weekend (mean ± 95% confidence interval).

located. Both gasoline vehicle and diesel emissions show weekday/weekend variations in Figure 6. The strong weekday-high variations of diesel emissions suggests the assignment to vehicles operating primarily on weekdays (Lewis et al. 2003). The ratio of the average contributions of diesel emissions relative to gasoline vehicle of 2.3 (= 1.88 μg/m^3 diesel emissions/ 0.83 μg/m^3 gasoline vehicle emissions) is consistent, with modeled ratios of 2.3 in Atlanta (Kim et al. 2004) and slightly lower than 3.2 in Pasadena, 3.0 in west Los Angeles (Schauer et al. 1996). The CMB study estimated a 3.2 μg/m^3 contribution from motor vehicle sources (Chow et al. 1998). The sum of mass contributions from gasoline vehicle and diesel emissions is 2.7 μg/m^3 and 2.0 μg/m^3 in this study and the PMF2 study (Maykut et al. 2003), respectively. Gasoline vehicles and diesel emissions contributed more to the $PM_{2.5}$ mass in the winter, as shown in Figure 5. The observed seasonal variations are

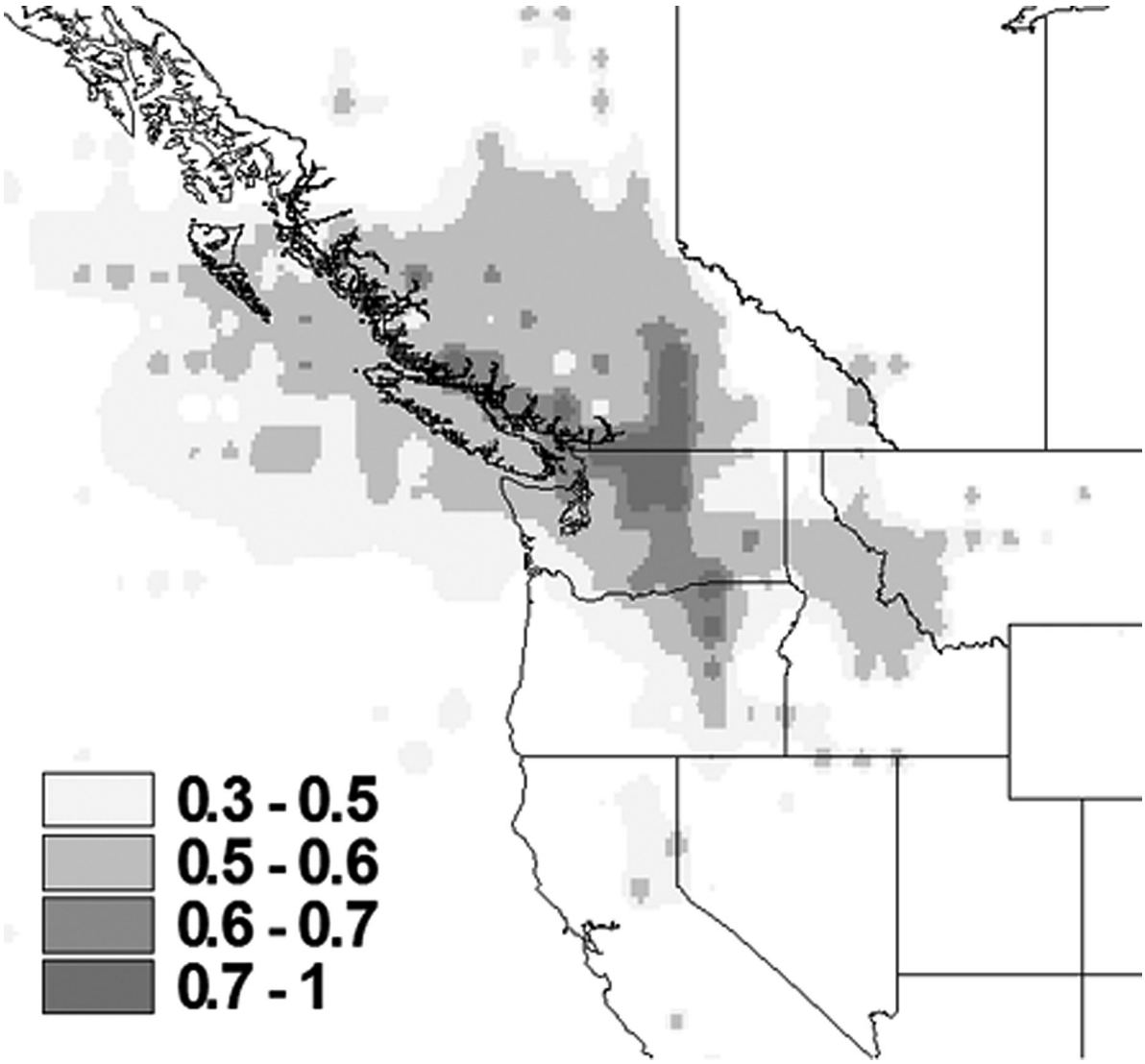

Figure 7. Potential source contribution function plot for the sulfate-rich secondary aerosol source.

probably due mainly to increased condensation of semivolatile compounds in winter as well as reduced mixing and dilution in the mixing layer during the frequent winter stagnation in Seattle.

The measured carbon fraction profiles from the source test reveals that the measured gasoline vehicle emissions have a large amount of OC4 and the diesel emissions contain high concentration of EC2 (Watson et al. 1994; Lowenthal et al. 1994). In contrast, the ME-derived carbon fraction profiles of this study have large amounts of OC3 and OC4 for the gasoline vehicle emissions and EC1 for the diesel emissions. The change in the evolution of carbon fractions in the thermal analysis may be influenced by the presence of other aerosol constituents. Transition metal oxides in the atmospheric aerosol may catalyze the oxidation of OC and EC fractions at a lower temperature, which results in higher concentrations of OC3 for the gasoline vehicle emissions and EC1 for the diesel emissions (Fung et al. 2002).

Wood smoke is characterized by OC and K (Watson et al. 2001) contributing 16% (1.4 μg/m^3) to the $PM_{2.5}$ mass concentration. This source is highly correlated with As (*Pearson correlation coefficients* = 0.90), which may be caused by the residential burning of wood scraps that were treated by chromated copper arsenate as a wood preservative. This high correlation was also reported in previously PMF2 study (Maykut et al. 2003). The CMB study identified a vegetative burning/cooking source contributing 1.8 μg/m^3 to the $PM_{2.5}$ mass concentration (Chow et al. 1998). The PMF2 study (Maykut et al. 2003) showed 2.5 μg/m^3 contribution of wood burning to the $PM_{2.5}$ mass concentration. This source profile has large amount of lower temperature carbon fractions (OC1–OC4), as shown in Figure 8. This source has a seasonal trend with higher values in

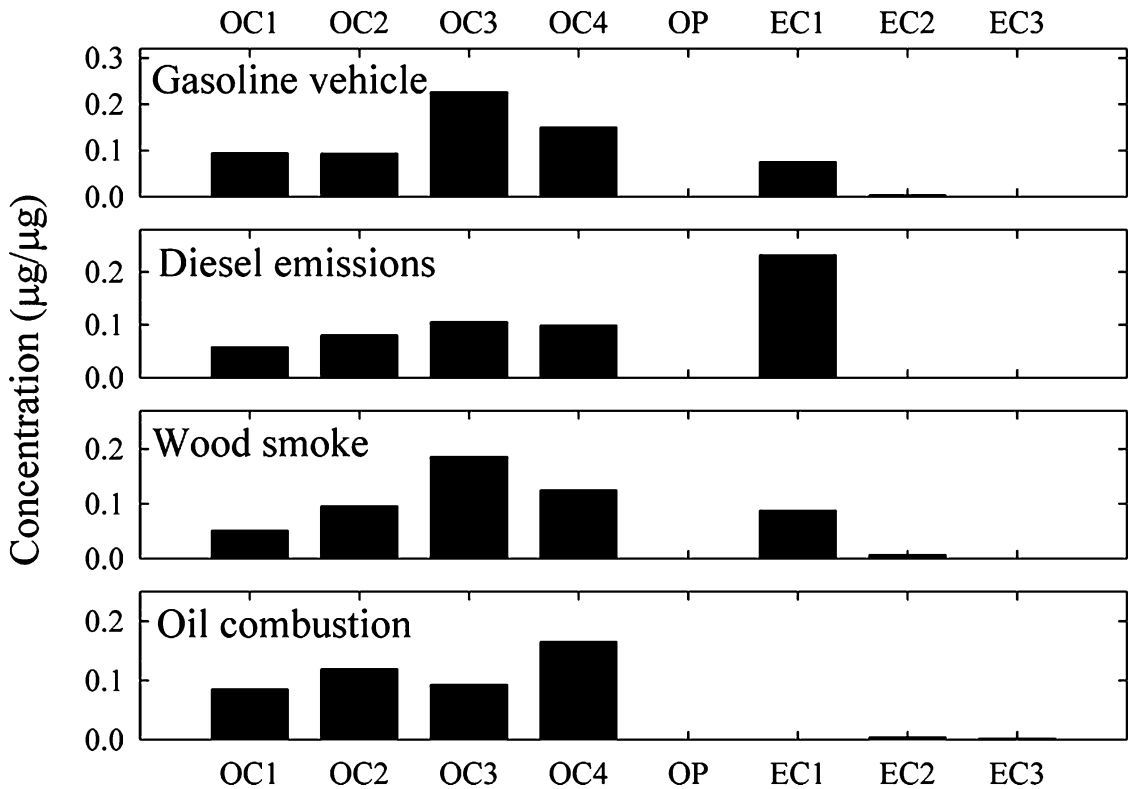

Figure 8. Fractional carbon profiles for combustion sources.

winter, suggesting residential wood burning. The CPF plot for wood smoke points to the north and east, where the residential areas are located.

Aged sea salt is suggested because the profile characterized by its high mass fraction of S, NO_3^-, Cl^-, and Na, which may be caused by chloride displacement by the acidic gases. This source accounts for 8% (0.7 $\mu g/m^3$) of the $PM_{2.5}$ mass concentration. The CMB study deduced $NaNO_3$ contributing 0.8 $\mu g/m^3$ to the $PM_{2.5}$ mass concentration (Chow et al. 1998). The PMF2 study showed 0.4 $\mu g/m^3$ contribution of aged sea salt that had high concentrations of NO_3^- and Na (Maykut et al. 2003). This source has a seasonal trend with slightly higher contributions in summer. In Figure 9, there are indications of higher contributions from the west in which the Pacific Ocean and Puget sound are situated.

Airborne soil is characterized by Si, Fe, Ca, Al, and K (Watson and Chow 2001; Watson et al. 2001) contributing 7% (0.6 $\mu g/m^3$) to the $PM_{2.5}$ mass concentration. The previous studies showed 0.3 $\mu g/m^3$ (Chow et al. 1998) and 1.2 $\mu g/m^3$ (Maykut et al. 2003) contributions of airborne soil to the $PM_{2.5}$ mass concentration. The airborne soil shows seasonal variation with higher concentrations in the relatively dry summer season. The carbon contents in this source and main contributions from northwest and west suggest that the airborne soil is mainly crustal particles resuspended by road traffic. The high contribution of this source on April 29, 1998 is the result of an Asian dust storm in western China and Gobi desert between 14 and 19 April, 1998 (Tratt et al. 2000; Vancuren et al. 2002).

The nitrate-rich secondary aerosol is represented by its high concentration of NO_3^-. This source accounts for 5% of the $PM_{2.5}$ mass concentration. This source was not resolved in the previous CMB and PMF studies (Chow et al. 1998; Maykut et al. 2003). This source does not have strong seasonal variations shown in Figures 4 and 5. In the studies of northeastern aerosols (Song et al. 2001) and southeastern aerosols (Kim et al. 2004), nitrate-rich secondary particles have a seasonal variation with maxima in winter, suggesting that low temperature and high relative humidity help the formation of nitrate aerosols in eastern U.S. In Seattle, the weak seasonal variation of nitrate-rich secondary aerosol is thought to be caused by low photochemical activity in winter in Seattle (Stein and Lamb 2003). The CPF plot shows the contributions from north. This direction is thought to indicate the contributions from downtown Seattle and highway junction between I-5 and I-90.

The sea salt is represented by its high concentration of Na and Cl^-, accounting for 4% of the $PM_{2.5}$ mass concentration. The 0.3 $\mu g/m^3$ average contribution of sea salt to the $PM_{2.5}$ mass concentration is consistent with 0.3 $\mu g/m^3$ resolved in the PMF2 study (Maykut et al. 2003). The CMB study also resolved 0.3 $\mu g/m^3$ contribution from marine sources (Chow et al. 1998). This source shows a winter-high seasonal pattern. In Figure 9, the CPF plot shows the contributions from the southwest, which

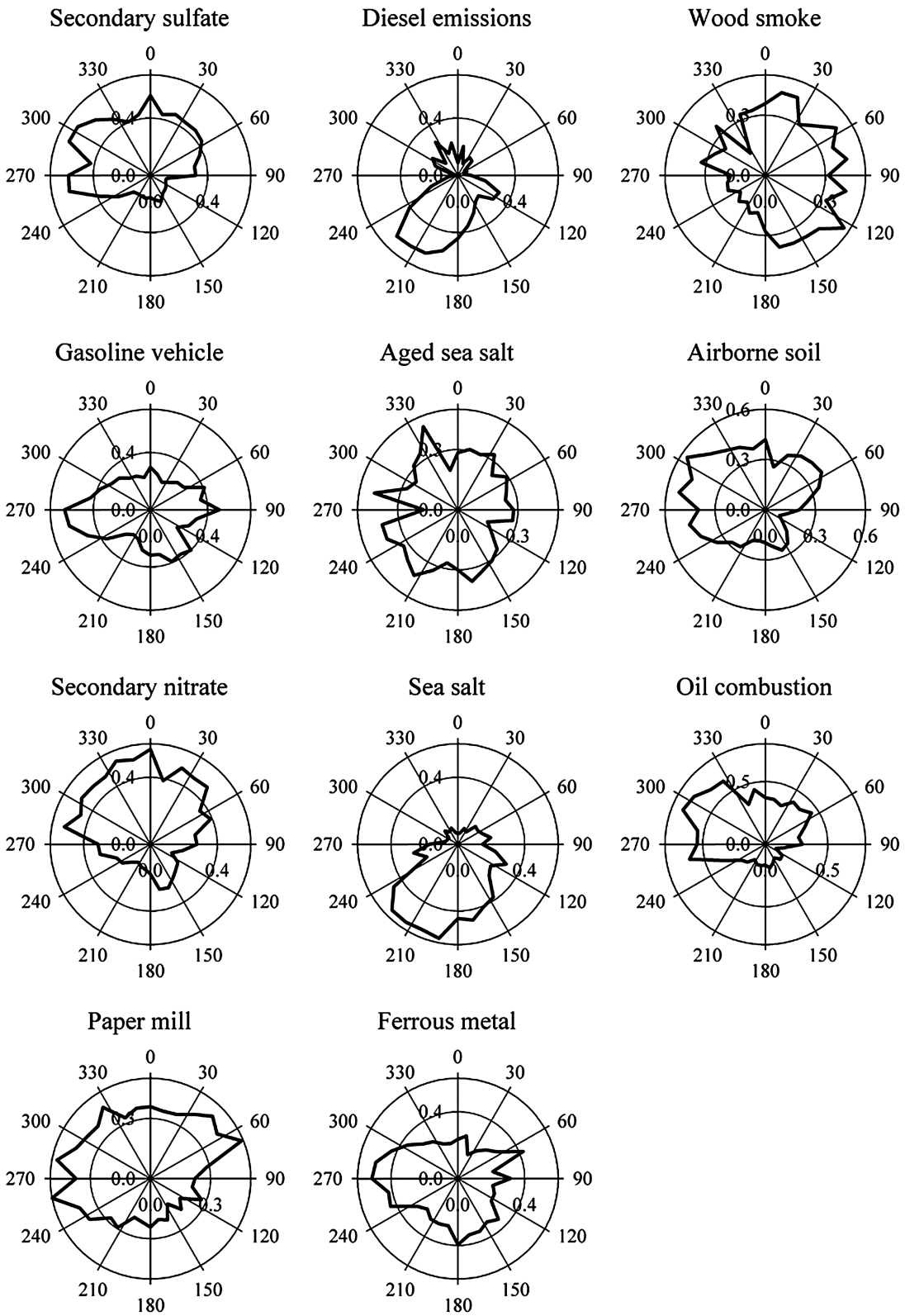

Figure 9. Conditional probability function plots for the highest 30% of the mass contributions.

is consistent with the direction of higher wind speed (upper 25%) at the Beacon Hill monitoring site.

Oil combustion is characterized by carbon fractions, V, and Ni. This source contributes 3% (0.2 $\mu g/m^3$) to the $PM_{2.5}$ mass concentration. The previous Seattle aerosol studies estimated 0.1 $\mu g/m^3$ (Chow et al. 1998) and 0.9 $\mu g/m^3$ (Maykut et al. 2003) contributions to the $PM_{2.5}$ mass concentration. As shown in Figure 8, this source profile has large amount of OC4 carbon fractions, reflecting residual oil combustion for the utilities and industries. The CPF plot of this source in Figure 9 points to the northwest, indicating downtown Seattle and the Port of Seattle as major contributors of this source. The impacts of oil combustion shows a summer-high seasonal trend in Figure 5 and does not show weekday/weekend variations, as shown in Figure 6.

In this study, two industrial point sources were extracted that were not resolved in the PMF2 study (Maykut et al. 2003). A paper mill profile is identified by Na and K (USEPA 2002) contributing 2% (0.2 $\mu g/m^3$) to the $PM_{2.5}$ mass concentration. The CPF plot for the paper mill in Figure 9 points to the west, northwest, and northeast, where paper and pulp mills are located. Ferrous-metal–processing is identified by its high mass fractions of Fe, Mn, Si, Ca, Cr, and Cu (USEPA 2002). This source accounts for 1% (0.1 $\mu g/m^3$) of the $PM_{2.5}$ mass concentration. In Figure 9, there are indications of higher contributions from the west and south, suggesting the specific ferrous-metal–processing plant located about 5 km west of the site, as well as several facilities located south of the site. These two industrial point sources do not show a strong seasonal pattern. The ferrous metal processing does show a strong weekday-high variation. The CMB study attributed 0.1 $\mu g/m^3$ and 0.2 $\mu g/m^3$ of the $PM_{2.5}$ mass concentration to the paper mill and metal processing sources, respectively (Chow et al. 1998).

CONCLUSION

Integrated $PM_{2.5}$ compositional data from samples collected at an urban monitoring site in Seattle, Washington were analyzed using a different least-squares program, ME. The ME solution provided an enhanced source resolution, including two industrial point sources and the nitrate-rich aerosol source, which were not deduced by a previous PMF2 study of the Seattle aerosol (Maykut et al. 2003). The gasoline vehicle emissions show carbon fractions without significant EC. Diesel emissions contain high concentrations of the EC fractions. Sulfate-rich secondary aerosols and diesel emissions are two largest $PM_{2.5}$ sources at the Beacon Hill monitoring site, accounting for 48% of the mass concentration. The impacts from local point sources are clearly seen using ME results combined with the CPF plots. The preliminary PSCF analysis indicates that southern Washington, along the Canadian border, and southwestern British Colombia, Canada are the possible source areas and pathways of the sulfate-rich secondary aerosols that impact on Beacon Hill monitoring site during the study period.

REFERENCES

Ashbaugh, L. L., Malm, W. C., and Sadeh, W. Z. (1985). A Residence Time Probability Analysis of Sulfur Concentrations at Grand Canyon National Park, *Atmos. Environ.* 19(8):1263–1270.

Cahill, T. A., Elred, R. A., Wallace, D. D., and Kusco, B. H. (1987). The Hydrogen-Sulfur Correlation, by PIXE plus PESA, and Aerosol Source Identification, *Nucl. Instrum. Methods Phys. Res.* B22:296–300.

Chow, J. C., and Watson, J. G. (1998). *Western Washington 1996–97 $PM_{2.5}$ Source Apportionment Study*. Final Report No. 98-01 Puget Sound Air Pollution Control Agency, Seattle, WA.

Chow, J. C., Watson, J. G., Pritchett, L. C., Pierson, W. R., Frazier, C. A., and Purcell, R. G. (1993). The DRI Thermal/Optical Reflectance Carbon Analysis System: Description, Evaluation and Applications in U.S. Air Quality Studies, *Atmos. Environ.* 27A(8):1185–1201.

Draxler, R. R., and Rolph, G. D. (2003). *HYSPLIT (HYbrid Single-Particle Lagrangian Integrated Trajectory) Model Access via NOAA ARL READY Website* (*http://www.arl.noaa.gov/ready/ hysplit4.html*). NOAA Air Resources Laboratory, Silver Spring, MD.

Fung, K., Chow, J. C., and Watson, J. G. (2002). Evaluation of OC/EC Speciation by Thermal Manganese Dioxide Oxidation and the IMPROVE Method, *J. Air Waste Manag. Assoc.* 52:1333–1341.

Henry, R. C. (1987). Current Factor Analysis Models are Ill-Posed, *Atmos. Environ*. 21:1815–1820.

Henry, R. C., and Norris, G. A. (2002). *EPA Unmix 2.3 User Guide*. http://www.epa.gov/ttn/amtic/unmixmtg.html

Hopke, P. K. (1985). *Receptor Modeling in Environmental Chemistry*. John Wiley & Sons, New York.

Hopke, P. K., Barrie, L. A., Li, S. M., Cheng, M. D., Li, C., and Xie, Y. L. (1995). Possible Sources and Preferred Pathways for Biogenic and Non-Sea Salt Sulfur for the High Arctic, *J. Geophys. Res.* 100(D8):16595–16603.

Hopke, P. K., Ramadan, Z., Paatero, P., Norris, G., Landis, M. S., Williams, R. W., and Lewis, C. W. (2003). Receptor Modeling of Ambient and Personal Exposure Samples: 1998 Baltimore Particulate Matter Epidemiology-Exposure Study, *Atmos. Environ.* 37:3289–3302.

Huang, S., Rahn, K. A., and Arimoto, R. (1999). Testing and Optimization Two Factor-Analysis Techniques on Aerosol at Narragansett, Rhode Island, *Atmos. Environ.* 33:2169–2185.

Kim, B. M., and Henry, R. C. (2000). Application of the SAFER Model to Los Angeles PM_{10} Data, *Atmos. Environ.* 34:1747–1759.

Kim, E., Hopke, P. K., and Edgerton, E. S. (2004). Improving Source Identification of Atlanta Aerosol Using Temperature Resolved Carbon Fractions in Positive Matrix Factorization, *Atmos. Environ.* 38:3349–3362.

Kim, E., Hopke, P. K., and Edgerton, E. S. (2003a). Source Identification of Atlanta Aerosol by Positive Matrix Factorization, *J. Air Waste Manag. Assoc.* 53:731–739.

Kim, E., Hopke, P. K., Paatero, P., and Edgerton, E. S. (2003b). Incorporation of Parametric Factors into Multilinear Receptor Model Studies of Atlanta Aerosol, *Atmos. Environ.* 37:5009–5021.

Kim, E., Larson, T. V., Hopke, P. K., Slaughter, C., Sheppard, L. E., and Claiborn, C. (2003c). Source Identification of $PM_{2.5}$ in an Arid Northwest U.S. City by Positive Matrix Factorization, *Atmos. Res.* 66:291–305.

Lewis, C. W., Norris, G. A., Conner, T. L., and Henry, R. C. (2003). Source Apportionment of Phoenix $PM_{2.5}$ Aerosol with the Unmix Receptor Model, *J. Air Waste Manag. Assoc.* 53:325–338.

Liu, D., Wenzel, R. J., and Prather, K. A. (2003). Aerosol Time-of-Flight Mass Spectrometry During the Atlanta Supersite Experiment: 1. Measurements, *J. Geophys. Res.* 108(D7):8426.

Lowenthal, D. H., Zielinska, B., Chow, J. C., and Watson, J. G. (1994). Characterization of Heavy Duty Diesel Vehicle Emissions, *Atmos. Environ*. 28(4):731–743.

Malm, W. C., Sisler, J. F., Huffman, D., Eldred, R. A., and Cahill, T. A. (1994). Spatial and Seasonal Trends in Particle Concentration and Optical Extinction in the United Sates, *J. Geophys. Res.* 99(D1):1347–1370.

Maykut, N. N., Lewtas, J., Kim, E., and Larson, T. V. (2003). Source Apportionment of $PM_{2.5}$ at an Urban IMPROVE Site in Seattle, WA, *Environ. Sci. Technol.* 37(22):5135–5142.

Miller, M. S., Friedlander, S. K., and Hidy, G. M. (1972). A Chemical Element Balance for the Pasadena Aerosol, *J. Colloid Interface Sci.* 39:165–176.

Paatero, P. (1997). Least Square Formulation of Robust Non-Negative Factor Analysis, *Chemometrics Intelligent Lab. Syst.* 37:23–35.

Paatero, P. (1999). The Multilinear Engine-A Table Driven, Least Square Program for Solving Multilinear Problems, Including the n-way Parallel Factor Analysis Model, *J. Computational Graphical Stat.* 8(4):854–888.

Paatero, P. (2000). *User's Guide for Positive Matrix Factorization Programs PMF2 and PMF3, Part 1: Tutorial.* ftp://ftp.clarkson.edu/pub/hopkepk/pmf/

Paatero, P., and Hopke, P. K. (2003). Discarding or Downweighting High-Noise Variables in Factor Analytic Models, *Analytica Chimica Acta* 490:277–289.

Pankow, J. F., and Mader, B. T. (2001). Gas/Solid Partitioning of Semivolatile Organic Compounds (SOCs) to Air Filters. 3. An Analysis of Gas Adsorption Artifacts in Measurements of Stmospheric SOCs and Organic Carbon (OC) when Using Teflon Membrane Filters and Quartz Fiber Filters, *Environ. Sci. Technol.* 35(17):3422–3432.

Poirot, R. L., Wishinski, P. R., Hopke, P. K., and Polissar, A. V. (2001). Comparative Application of Multiple Receptor Methods to Identify Aerosol Sources in Northern Vermont, *Environ. Sci. Technol.* 35(23):4622–4636.

Polissar, A. V., Hopke, P. K., and Harris, J. M. (2001b). Source Regions for Atmospheric Aerosol Measured at Barrow, Alaska, *Environ. Sci. Technol.* 35:4214–4226.

Polissar, A. V., Hopke, P. K., Paatero, P., Malm, W. C., and Sisler, J. F. (1998). Atmospheric Aerosol Over Alaska 2. Elemental Composition and Sources, *J. Geophys. Res.* 103(D15):19045–19057.

Polissar, A. V., Hopke, P. K., and Poirot, R. L. (2001a). Atmospheric Aerosol Over Vermont: Chemical Composition and Sources, *Environ. Sci. Technol*. 35:4604–4621.

Qin, Y., Oduyemi, K., and Chan, L. Y. (2002). Comparative testing of PMF and CFA Models, *Chemometrics Intelligent Lab. Syst.* 61:75–87.

Ramadan, Z., Eickhout, B., Song, X. H., Buydens, L., and Hopke, P. K. (2003). Comparison of Positive Matrix Factorization (PMF) and Multilinear Engine (ME-2) for the Source Apportionment of Particulate Pollutants, *Chemometrics Intelligent Lab. Syst.* 66(1):15–28.

Ramadan, Z., Song, X. H., and Hopke, P. K. (2000). Identification of Sources of Phoenix Aerosol by Positive Matrix Factorization, *J. Air Waste Manag. Assoc.* 50:1308–1320.

Rolph, G. D. (2003). *Real-time Environmental Applications and Display sYstem (READY) Website* (*http://www.arl.noaa.gov/ready/hysplit4.html*). NOAA Air Resources Laboratory, Silver Spring, MD.

Schauer, J. J., Rogge, W. F., Hildemann, L. M., Mazurek, M. A., and Cass, G. R. (1996). Source Apportionment of Airborne Particulate Matter using Organic Compounds as Tracers, *Atmos. Environ.* 30:3837–3855.

Song, X. H., Polissar, A. V., and Hopke, P. K. (2001). Source of Fine Particle Composition in the Northeastern US, *Atmos. Environ.* 35:5277–5286.

Stein, A. F., and Lamb, D. (2003). Empirical Evidence for the Low- and High-NOx Photochemical Regimes of Sulfate and Nitrate Formation, *Atmos. Environ.* 37:3615–3625.

Tratt, D. M., Frouin, R. J., and Westphal, D. L. (2000). April 1998 Asian Dust Event: A Southern California Perspective, *J. Geophys. Res.* 106(18):371–380.

US EPA. 2002. *SPECIATE Version 3.2.* US Environmental Protection Agency, Research Triangle Park, NC.

Vancuren, R. A., and Cahill, T. A. (2002). Asian Aerosols in North America: Frequency and Concentration of Fine Dust, *J. Geophys. Res.* 107(D24):4804.

Washington State Department of Transportation. (2002). 2001 Annual Traffic Report. Washington State, Olympia, Washington.

Watson, J. G., and Chow, J. C. (2001). Source Characterization of Major Emission Sources in the Imperial and Mexicali Valleys Along the US/Mexico Border, *Sci. Total Environ.* 276:33–47.

Watson, J. G., Chow, J. C., and Houck, J. E., (2001). $PM_{2.5}$ Chemical Source Profiles for Vehicle Exhaust, Vegetative Burning, Geological Material, and Coal Burning in Northwestern Colorado During 1995, *Chemosphere* 43:1141–1151.

Watson, J. G., Chow, J. C., Lowenthal, D. H., Pritchett, L. C., and Frazier, C. A. (1994). Differences in the Carbon Composition of Source Profiles for Diesel and Gasoline Powered Vehicles, *Atmos. Environ.* 28(15):2493–2505.

Willis, R. D. (2000). *Workshop on UNMIX and PMF as applied to* $PM_{2.5}$. EPA 600-A-00-048.

Xie, Y. L., Hopke, P. K., Paatero, P., Barrie, L. A., and Li, S. M. (1999). Identification of Source Nature and Seasonal Variations of Arctic Aerosol by the Multilinear Engine, *Atmos. Environ*. 33:2549–2562.

Yli-Tuomi, T., Hopke, P. K., Paatero, P., Basumia, M. S., Landsberger, S. L., Viisanen, Y., and Paatero, J. (2003). Atmospheric Aerosol Over Finnish Arctic: Source Analysis by the Multilinear Engine and the Potential Source Contribution Function, *Atmos. Environ.* 37:4381–4392.